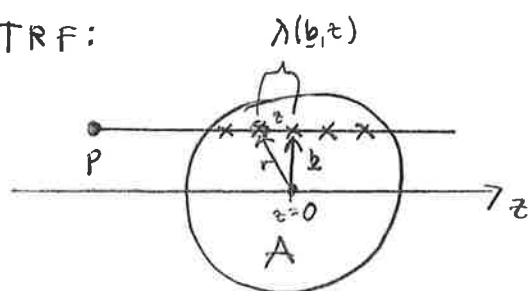


6. Nuclear collision geometry: $N_{bin}^{AA}(\underline{b})$, $N_{part}^{AA}(\underline{b})$, centrality

The high-energy picture of $A+B$ collision $\hat{=}$ eikonal approximation, where the nucleons collide several times and move along a straight path.

A. $p+A$ collision

in TRF:



\underline{b} = impact parameter ($\underline{b} \perp$ plane), often taken to define the x -axis

Assume: the amount ΔE the projectile p loses in each collision is small: $\frac{\Delta E}{\sqrt{s_{NN}}} \ll 1$ & high nuclear transparency

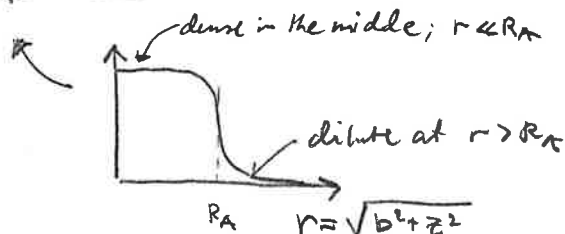
\Rightarrow $\left\{ \begin{array}{l} \text{the subcollisions } pN \approx \text{identical;} \\ p \text{ moves from one collision to the next one along straight line trajectory} \end{array} \right.$

The mean free path between the subcollisions is

$$\lambda(\underline{b}, z) = \frac{1}{n_A(\underline{b}, z) \sigma_{NN}(\sqrt{s_{NN}})}$$

nuclear matter density of target A

σ_{NN} cross section of NN scattering; unchanged from collision to collision ($\sigma_{pp} \approx \sigma_{pn} \approx \sigma_{nn}$ now)



R_A = the radius of nucleus A

The average number of binary $\sqrt{s_{NN}}$ collisions in a pA collision at $\sqrt{s_{NN}}$ at a fixed impact parameter \underline{b} :

$$N_{bin}^{pA}(\underline{b}) = \int_{-\infty}^{\infty} \frac{dz}{\lambda(\underline{b}, z)} = \int_{-\infty}^{\infty} dz n_A(\underline{b}, z) \sigma_{NN}(\sqrt{s_{NN}}) = T_A(\underline{b}) \sigma_{NN}(\sqrt{s_{NN}})$$

where

$$T_A(\underline{b}) \equiv \int_{-\infty}^{\infty} dz n_A(\underline{b}, z) \text{ is the nuclear thickness function}$$

Normalization:

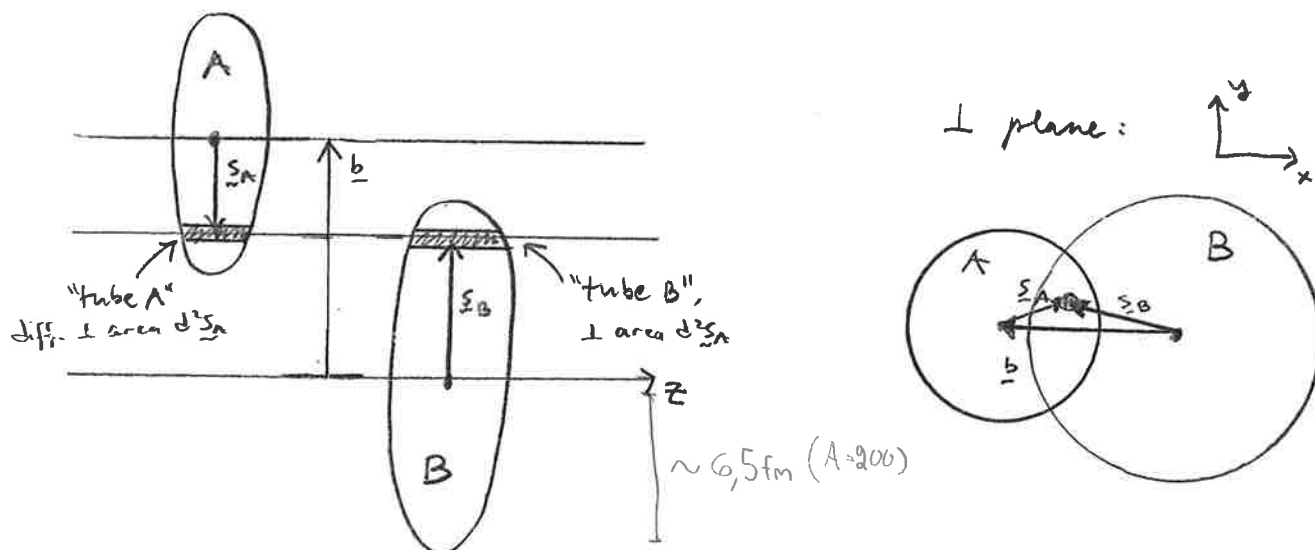
$$\int d^2b T_A(\underline{b}) = \int \underbrace{d^2b}_{d^2r} dz n_A(\underline{r}) = A$$

-178-

Thus $N_{bin}^{pA} \sim T_A \sim A^{1/3}$.

B. $A+B$ collision

\underline{b} = impact parameter



The number of nucleons in tube A: $dn_A = d^2s_A \int_{-\infty}^{\infty} dz n_A(\underline{s}_A, z)$
 $= d^2s_A T_A(\underline{s}_A)$

Generalize from the pA case: all dn_A nucleons in the tube A collide with the nucleons in the tube B; the average number of binary NN collisions in the collision of tubes A & B:

$$dN_{bin}^{AB}(\underline{s}_A, \underline{s}_B, \underline{b}) = dn_A(\underline{s}_A) \cdot N_{bin}^{pB}(\underline{s}_B = \underline{b} + \underline{s}_A)$$

$$= d^2s_A T_A(\underline{s}_A) T_B(\underline{b} + \underline{s}_A) \sigma_{NN}(\sqrt{s_{NN}})$$

the average number of binary NN collisions in an AB collision at $\sqrt{s_{NN}}$ and a fixed impact parameter \underline{b} :

$$N_{bin}^{AB}(\underline{b}) = \int d^2s_A T_A(\underline{s}_A) T_B(\underline{b} + \underline{s}_A) \cdot \sigma_{NN}(\sqrt{s_{NN}}) = T_{AB}(\underline{b}) \sigma_{NN}(\sqrt{s_{NN}})$$

where

$$T_{AB}(\underline{b}) \equiv \int d^2s T_A(\underline{s}) T_B(\underline{b} + \underline{s})$$

is the nuclear overlap function

We consider spherical nuclei; for these $T_A(z) = T_A(-z)$, and $T_{AB}(z)$ is often expressed as

$$T_{AB}(z) = \int d^2s \, T_A(z) T_B(b-z)$$

There are a few special cases which give analytical solutions for T_A & T_{AB} . The relevant ones can be found in the Appendix of Eskola, Kajantie, Lindfors, Nucl. Phys. B 323 (1989) 27, see the pages 180-182 below.

Normalization:

$$\begin{aligned} \int d^2b \, T_{AB}(b) &= \int d^2b \int d^2s \, T_A(z) T_B(b-z) = AB \\ &= \underbrace{\int d^2b' \, T_B(b')}_B \underbrace{\int d^2s \, T_A(z)}_A \end{aligned}$$

G. Glauber geometry for A+B

(Glauber = Nobelist '05!)

Let's consider inelastic AB collision. The maximum number of binary NN collisions is AB (all N in A collide with all N in B). Out of these, there are N inelastic NN collisions ($N=1, \dots, AB$)

↑
at least one, since we have an inelastic AB collision

Formulate a binomial probability distribution for having N inelastic collisions in an AB collision at a fixed impact parameter b :

$$P(N, b) = \binom{AB}{N} \left(\frac{T_{AB}(b) G_{NN}^{\text{in}}}{AB} \right)^N \left(1 - \frac{T_{AB}(b) G_{NN}^{\text{in}}}{AB} \right)^{AB-N}$$

ways to choose N inelastic collisions out of all AB NN collisions

probability of having an inelastic NN collision at $\sqrt{s_{NN}}, b$, is $\frac{T_{AB}(b) G_{NN}^{\text{in}}}{AB}$

probability of not having an inelastic NN collision

The above assumes that all NN subcollisions are independent.

($T_{AB}(b) G_{NN}^{\text{in}}$ is the average number of inelastic NN collisions† at $\sqrt{s_{NN}}$ and b)

approximately few hundreds of hard quarks and gluons are produced in a time $1/p_0 \approx 0.1$ fm after the collision. What happens to these partons before the soft hadronic time scale ≈ 1 fm? Preliminary estimates indicate that collisions even among the constituents of this subsystem will drive this subsystem towards thermalisation. Thermalisation is all the more likely if interactions with the soft component are included. It would also be interesting to compute how many dileptons are produced during this pre-equilibrium stage and compare the result with both the instantaneous Drell-Yan rate and the later thermal dilepton production.

We thank S. Ellis for discussions. K.J.E. and K.K. thank the Academy of Finland for financial support.

Appendix. Nuclear geometry

Here we shall collect a few formulas relevant for the inclusion of the effects of nuclear geometry for spherically symmetric nuclei in very high energy heavy ion collisions. The relevant quantities are

1. The nuclear density:

$$n_A(r), \quad \int d^3r n_A(r) = A. \quad (\text{A.1})$$

2. The thickness function:

$$T_A(b) = \int_{-\infty}^{\infty} dz n_A(\sqrt{b^2 + z^2}), \quad (\text{A.2})$$

$$\int d^2b T_A(b) = A, \quad (\text{A.3})$$

where z is the longitudinal coordinate and \vec{b} is a two-dimensional vector in the transverse plane, $b = |\vec{b}|$.

3. The overlap function:

$$T_{AB}(b) = \int d^2b_1 d^2b_2 \delta^2(\vec{b} - \vec{b}_1 - \vec{b}_2) T_A(\vec{b}_1) T_B(\vec{b}_2), \quad (\text{A.4})$$

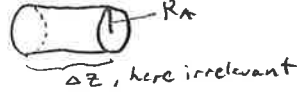
$$\int d^2b T_{AB}(b) = AB. \quad (\text{A.5})$$

Physically, $\sigma T_A(b)(\sigma T_B(b))$, where σ is an $N + N$ cross section, gives the number of $N + N$ collisions where a nucleon crosses a nucleus (nucleus A crosses the nucleus

B) at impact parameter b . The natural magnitudes of $T_A(b)$ and $T_{AB}(b)$ are $A/\pi R_A^2$ and $AB/\pi(R_A + R_B)^2$, respectively.

There are a few special cases in which some of the integrals can be done analytically:

Cylindrical nuclei:



$$T_A(b) = \frac{A}{\pi R_A^2} \Theta(R_A^2 - b^2), \quad T_{AB}(b) = \frac{A}{\pi R_A^2} \frac{B}{\pi R_B^2} \mathcal{A}(b), \quad (\text{A.6, A.7})$$

where $\mathcal{A}(b)$ is the overlap area of two discs at a distance b (choosing $R_A < R_B$):

$$\mathcal{A} = \pi R_A^2, \quad b < R_B - R_A,$$

$$(\text{E}_{\times}) \quad = R_B^2 \arccos \frac{b^2 + R_B^2 - R_A^2}{2bR_B} + R_A^2 \arccos \frac{b^2 + R_A^2 - R_B^2}{2bR_A} - \frac{1}{2} \sqrt{-\lambda},$$

$$R_B - R_A < b < R_B + R_A,$$

$$= 0, \quad R_A + R_B < b, \quad (\text{A.8})$$

where $\lambda \equiv (b^2 - R_A^2 - R_B^2)^2 - 4R_A^2 R_B^2$.

Sphere with sharp surface:



$$n_A(r) = \frac{3}{4} \frac{A}{\pi R_A^3} \Theta(R_A^2 - r^2), \quad (\text{A.9})$$

$$(\text{E}_{\times}) \quad T_A(b) = \frac{3}{2} \frac{A}{\pi R_A^2} \sqrt{1 - b^2/R_A^2} \Theta(R_A^2 - b^2), \quad (\text{A.10})$$

$$T_{AA}(0) = \frac{9}{8} \frac{A^2}{\pi R_A^2}. \quad (\text{A.11})$$

Woods-Saxon distribution [30]: ^{Bohr & Mottelson, Nuclear Structure I (Benjamin, NY 1969) p. 160, 222,}

$$n_A(r) = n_0 / [1 + e^{(r-R_A)/d}], \quad (\text{A.12})$$

where, neglecting terms of the order of $\exp(-R_A/d)$, $n_0 \approx 0.17/\text{fm}^3$ is the central density and $d = 0.54 \text{ fm}$ is the thickness. The normalisation (A.1) relates the parameters as follows: (E_{\times})

$$n_0 = \frac{3}{4} \frac{A}{\pi R_A^3} \frac{1}{1 + \pi^2 d^2 / R_A^2} \quad (\text{A.13})$$

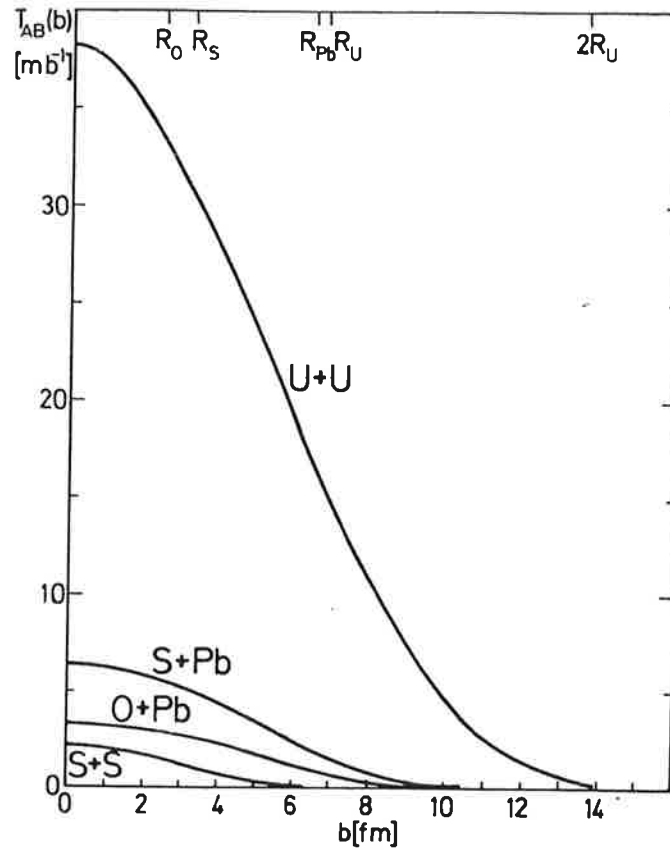


Fig. 8. $T_{AB}(b)$ given by eq. (A.4) computed for the Woods-Saxon distribution (A.12) for U + U, S + Pb, O + Pb and S + S collisions (U = 238, Pb = 208, S = 32, O = 16). The values of $T_{AB}(0)$ are 38.2, 6.39, 3.29 and 2.19 mb^{-1} , respectively.

and from this one can solve (ϵ_{\times})

$$R_A = 1.12A^{1/3} - 0.86A^{-1/3} \text{ fm.} \quad (\text{A.14})$$

For $A \geq 16$ a numerically equivalent solution [31] is $R_A = 1.18A^{1/3} - 0.45 \text{ fm}$. One can compute analytically (ϵ_{\times})

$$T_A(0) = 2n_0d \ln(1 + e^{R_A/d}) \approx 2R_An_0, \quad (\text{A.15})$$

numerical evaluations are shown in fig. 8. Observe that for $A \approx 200$ $T_{AA}(0)$ is about $1.0A^2/\pi R_A^2$ while it is less for smaller nuclei; eq. (A.11) is approached for $R_A \gg d$.

↑ useful to remember

References

- [1] H. Satz, H.J. Specht and R. Stock, eds., Proc. of Quark Matter '87, Z. Phys. C38 (1988) 1
- [2] G. Baym, P. Braun-Munzinger and S. Nagamiya, eds., Proc. of Quark Matter '88, Nucl. Phys. A498 (1989)

The inelastic cross section of an AB collision becomes then (Ex.) -183-

$$\sigma_{in}^{AB} = \int d^2b \sum_{N=1}^{AB} P(N, \underline{b}) = \int d^2b \left\{ 1 - \left(1 - \frac{T_{AB}(\underline{b}) \sigma_{NN}^{in}}{AB} \right)^{AB} \right\}$$

not 0 but 1.

This is often referred to as the optical Glauber model for nuclear collisions.

probability of having at least 1 inelastic collision

Since $AB \rightarrow \infty$, we can also write

$$\sigma_{in}^{AB} = \int d^2b \left\{ 1 - \left(1 - \frac{T_{AB}(\underline{b}) \sigma_{NN}^{in}}{AB} \right)^{AB} \right\} \stackrel{AB \rightarrow \infty}{\approx} \int d^2b \left\{ 1 - e^{-T_{AB}(\underline{b}) \sigma_{NN}^{in}} \right\}$$

writing $1 - e^{-T_{AB}(\underline{b}) \sigma_{NN}^{in}} = e^{-T_{AB}(\underline{b}) \sigma_{NN}^{in}} (e^{T_{AB}(\underline{b}) \sigma_{NN}^{in}} - 1)$

order of magnitude:

$$T_{AB}(0) \approx 0.30 \left(\frac{1}{mb} \right) \quad (A \sim 200)$$

$$\sigma_{NN}^{in} (RHIC) \approx 40 \text{ mb}$$

$$\Rightarrow T_{AB}(0) \sigma_{NN}^{in} (RHIC) \approx 1200 \gg 1$$

$$= \sum_{N=1}^{\infty} \frac{(T_{AB}(\underline{b}) \sigma_{NN}^{in})^N}{N!} e^{-T_{AB}(\underline{b}) \sigma_{NN}^{in}}$$

Poisson probability distribution

$$e^{-T_{AB}(\underline{b}) \sigma_{NN}^{in}} \hat{=} P(\text{no inelastic collisions})$$

By construction, we now have the average number of inelastic NN collisions at a fixed \underline{b} as:

$$\langle N(\underline{b}) \rangle = \sum_{N=1}^{AB} N P(N, \underline{b}) \stackrel{\text{Ex.}}{=} AB \cdot \frac{T_{AB}(\underline{b}) \sigma_{NN}^{in}}{AB} = T_{AB}(\underline{b}) \sigma_{NN}^{in}$$

binomial

$$\stackrel{AB \rightarrow \infty}{=} \sum_{N=1}^{\infty} N P(N, \underline{b}) \stackrel{\text{Poisson}}{=} T_{AB}(\underline{b}) \sigma_{NN}^{in}$$

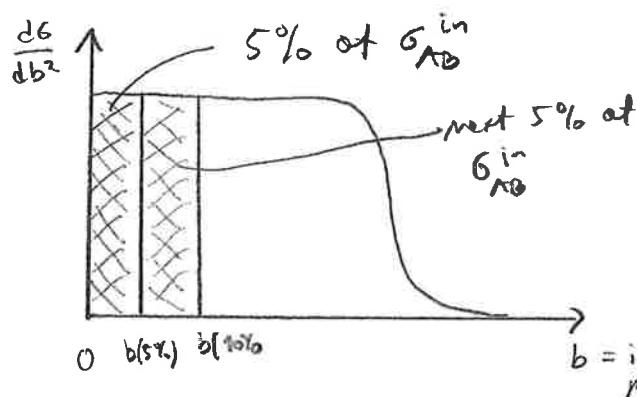
i.e.

$$\langle N(\underline{b}) \rangle = N_{bin;in}^{AB}(\underline{b})$$

With the optical Glauber cross section, we can see the effects of centrality (\underline{b}) and the effects of fluctuations.

D. Centrality in AB collisions & fluctuations in N_{ch}, E_T

let's define a centrality class in the Glauber model by looking percentages at σ_{AB}^{in}



$$\sigma_{AB}^{in} = \int d^2b \frac{d\sigma_{AB}^{in}}{d^2b} = \int d^2b \frac{\pi}{4} [1 - e^{-T_{AB}(b)\sigma_{NN}^{in}}]$$

"n% centrality class"
= "n% most central collisions"

$$\text{means } b^2(n\%)$$

$$\frac{n}{100} \sigma_{AB}^{in} = \int_0^{b^2(n\%)} d^2b \frac{1}{\pi} [1 - e^{-T_{AB}(b)\sigma_{NN}^{in}}]$$

$$\text{"5-10% centrality class"} \hat{=} 0.05 \sigma_{AB}^{in} = \int_{b^2(5\%)}^{b^2(10\%)} d^2b \frac{1}{\pi} [1 - e^{-T_{AB}(b)\sigma_{NN}^{in}}]$$

etc.

[Note: sometimes what is quoted for σ_{AB}^{in} is the "geometric cross section" ^{in the literature}
 $\sigma_{AB}^{in} = \pi(R_A + R_B)^2$ and the centrality classes are computed from this.]

In the experiments, however, life is not this easy:

for each b , there are fluctuations in N_{ch}, E_T, \dots

e.g. at PHENIX @ RHIC (see e.g. nucl-ex/0409015) one correlates forward and non-forward particle production to define centrality:

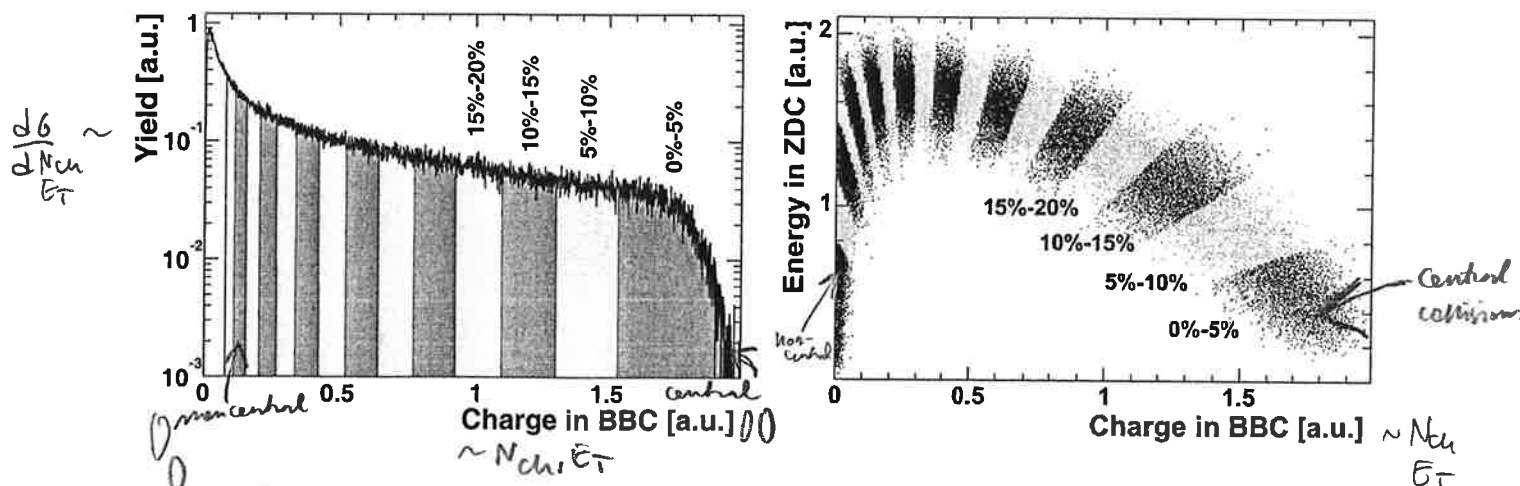


FIG. 1: Different centrality classes based on the BBC (left) and ZDC vs. BBC distributions (right).

BBC = beam-beam counter at $3.0 < |\eta| < 3.9$ $\hat{=}$ measures particle production; not forward
ZDC = zero-degree calorimeter at $|\eta| > 6$ $\hat{=}$ measures E of spectator neutrons; forward

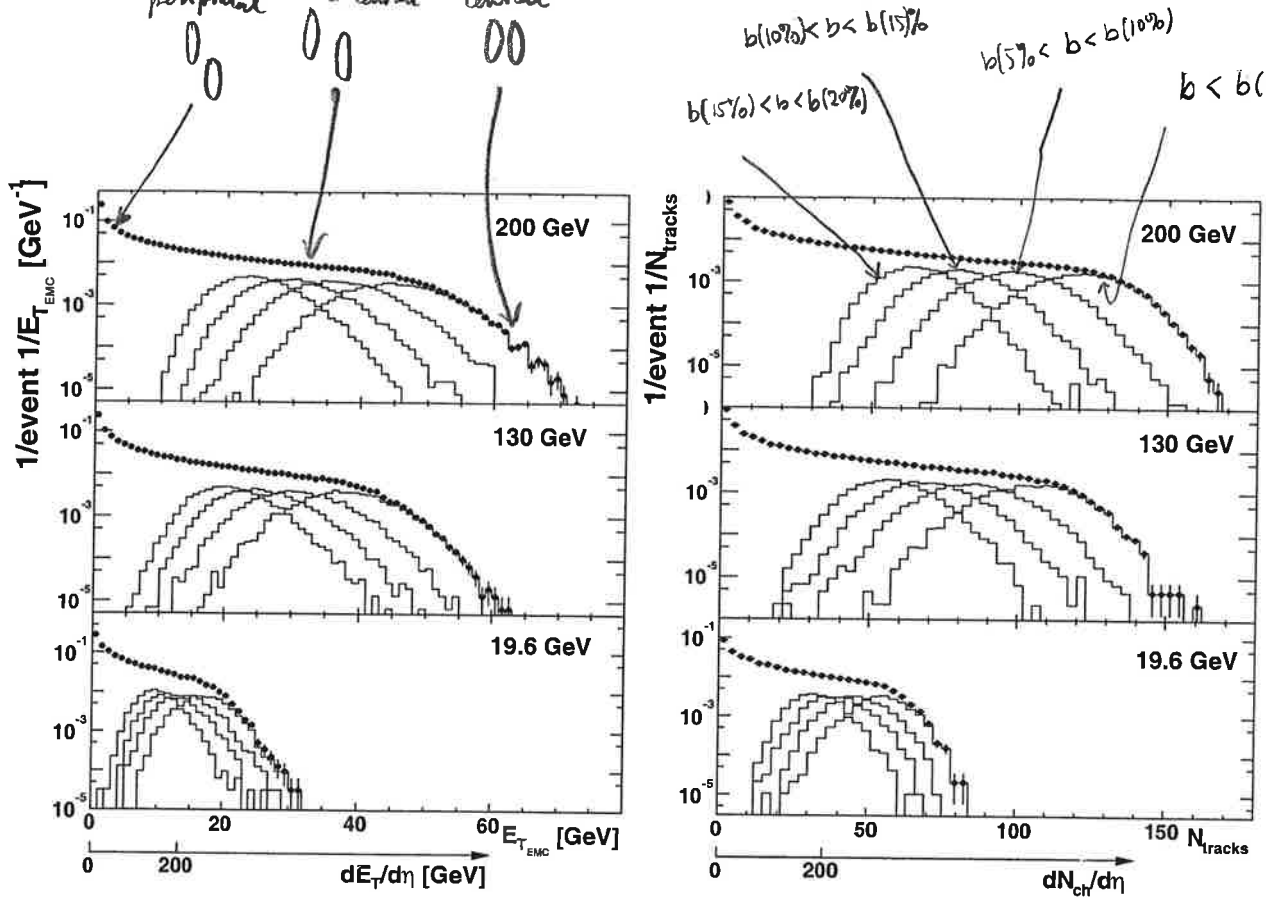


FIG. 4: The distribution of the raw E_T in two EMCAL sectors (left) and the number of tracks in the east arm of the PHENIX detector (right) per MB trigger, measured at three energies. The lower axis corresponds to mid-rapidity values of $dE_T/d\eta$ and $dN_{ch}/d\eta$ respectively. Distributions of the four 5% most central bins are also shown in each plot.

For the N_{ch} measurements at $\sqrt{s_{NN}} = 130$ GeV, only the east arm was used, while for the other two energies the measurements were made using both PHENIX central arms. The results obtained with two arms at $\sqrt{s_{NN}} = 200$ GeV and 19.6 GeV are consistent with each other within 1.5%.

The distributions shown in Fig. 4 have a characteristic shape with a sharp peak that corresponds to the most peripheral events. Missing events caused by the finite MB trigger efficiency in peripheral events would make this peak even sharper than measured. The plateau in all distributions corresponds to mid-central events and the fall-off to the most central $Au + Au$ events. The shape of the curves in Fig. 4 in the fall-off region is a product of the intrinsic fluctuations of the measured quantities and the limited acceptance of the detector.

The distributions for the four most central bins 0%-5% to 15%-20% are also shown in each panel. The centroids of these distributions were used to calculate the centrality dependence of $dE_T/d\eta$ and $dN_{ch}/d\eta$ ³. The statistical uncertainty of all mean values (less than or about 1%) determined by the width of the distributions are small because of the large size of the event samples.

The magnitude of $dE_T/d\eta$ and $dN_{ch}/d\eta$ at mid-rapidity divided by the number of participant pairs as a function of N_p is shown in Fig. 5 and tabulated in Tables XIII-XV. The right three panels show the same ratio for $dN_{ch}/d\eta$ at three RHIC energies.

The horizontal errors correspond to the uncertainty in N_p , determined within the framework of the Monte Carlo Glauber model. The vertical bars show the full systematic errors of the measurements⁴ added quadratically to the errors of N_p . The lines denote the corridor in which the points can be inclined or bent. The statistical errors are smaller than the size of the markers. The upper panel also shows the results of the two lower panels with open markers for comparison.

An important result from Fig. 5 is an evident consistency in the behavior of the centrality curves of E_T shown on the left and N_{ch} shown on the right for all measured energies. Both values demonstrate an increase from peripheral (65%-70% bin) to the most central events by 50%-70% at RHIC energies $\sqrt{s_{NN}} = 130$ GeV and 200 GeV. For the lowest RHIC energy ($\sqrt{s_{NN}} = 19.6$ GeV) this increase is at the level of systematic uncertainties of the measurement. One can note that results from PHO-

³ All plotted and quoted numbers correspond to average values in each centrality bin or ratios of those averages.

⁴ Here and everywhere errors correspond to one standard deviation.

from PHENIX,
mid-cx/0409015

To get an intuitive picture of the effect of fluctuations, let's consider the following simplified picture: see e.g. EKL, Nucl. Phys. B 323 (1989) 37

let's denote $N_{ch} \equiv \int dy \frac{dN_{charged}}{dy} = \# \text{ charged hadrons in, say, a (central) rapidity unit; } |y| \leq 0.5.$

In a NN collision the charged-particle distribution in inelastic collisions is $\frac{d\sigma_{NN}^{in}}{dN_{ch}}$ and we define the average as

$$\langle N_{ch}^{NN} \rangle = \frac{1}{\sigma_{NN}^{in}} \int dN_{ch} \frac{d\sigma_{NN}^{in}}{dN_{ch}} N_{ch}.$$

Assume that in an AB collision, the $N_{ch}^{AB} < N_{bin,in}^{AB}$, and that each NN subcollision contributes with the same # particles produced (this is not exactly true in a more realistic system). We can write:

$$\frac{d\sigma_{in}^{AB}}{dN_{ch}} = \int d^2b \sum_{N=1}^{\infty} P(N, b) \int dN_{ch1} dN_{ch2} \dots dN_{chN} \frac{1}{\sigma_{NN}^{in}} \frac{d\sigma_{NN}^{in}}{dN_{ch1}} \dots \frac{1}{\sigma_{NN}^{in}} \frac{d\sigma_{NN}^{in}}{dN_{chN}} \cdot \delta(N_{ch} - (N_{ch1} + N_{ch2} + \dots + N_{chN}))$$

normalization:

$$\int dN_{ch} \frac{d\sigma_{in}^{AB}}{dN_{ch}} = \sigma_{in}^{AB}$$

charged particles from collision 1 charged particles from collision 2 charged particles from coll. \rightarrow

Note especially that no QCD-matter effects are taken into account (in reality they must be taken into account, of course).

writing $\delta(N_{ch} - \sum_{k=1}^N N_{ch,k}) = \int_{-\infty}^{\infty} \frac{d\tau}{2\pi} e^{i\tau(N_{ch} - \sum_{k=1}^N N_{ch,k})}$, we get, using $P(N, b) = P(N, b)_{\text{Poisson}}$ p. 183

$$\frac{d\sigma_{in}^{AB}}{dN_{ch}} = \int d^2b \int_{-\infty}^{\infty} \frac{d\tau}{2\pi} e^{i\tau N_{ch}} e^{-N_{bin,in}^{AB}(b)} \sum_{N=1}^{\infty} \frac{[N_{bin,in}^{AB}(b)]^N}{N!} \cdot$$

$$\cdot \left[\frac{1}{\sigma_{NN}^{in}} \int dN_{ch1} \frac{d\sigma_{NN}^{in}}{dN_{ch1}} e^{-i\tau N_{ch1}} \right]^N$$

these integrals factorize, integrals identical

$$\text{write } \sum_{N=1}^{\infty} \frac{[N_{bin,in}^{AB}(b)]^N}{N!} \cdot \frac{1}{\sigma_{NN}^{in}} \int dN_{ch1} \frac{d\sigma_{NN}^{in}}{dN_{ch1}} e^{-i\tau N_{ch1}} = e^{N_{bin,in}^{AB}(b)} \frac{1}{\sigma_{NN}^{in}} \int dN_{ch1} \frac{d\sigma_{NN}^{in}}{dN_{ch1}} e^{-i\tau N_{ch1}} - 1$$

$$\Rightarrow \frac{dG_{in}^{AB}}{dN_{ch}} = \int d^2b \int \frac{d\tau}{2\pi} e^{i\tau N_{ch} + N_{bin,in}^{AB}(\underline{b})} \left\{ \frac{1}{G_{NN}^{in}} \int dN_{ch} \frac{dG_{NN}^{in}}{dN_{ch}} e^{-i\tau N_{ch}} - 1 \right\}$$

$$- \delta(N_{ch}) \int d^2b e^{-\bar{N}_{bin,in}^{AB}(\underline{b})}$$

P (no inelastic collisions)

where now $\frac{1}{G_{NN}^{in}} \int dN_{ch} \frac{dG_{NN}^{in}}{dN_{ch}} e^{-i\tau N_{ch}} - 1$

$$= \frac{1}{G_{NN}^{in}} \int dN_{ch} \frac{dG_{NN}^{in}}{dN_{ch}} \left[e^{-i\tau N_{ch}} - 1 \right] = -i\tau \langle N_{ch}^{NN} \rangle - \frac{\tau^2}{2} \langle N_{ch}^{NN2} \rangle$$

$$= -i\tau N_{ch} - \frac{\tau^2}{2} N_{ch}^2 + O(\tau^3) \quad 0$$

$$\Rightarrow \frac{dG_{in}^{AB}}{dN_{ch}} = \int d^2b \int \frac{d\tau}{2\pi} e^{i\tau N_{ch} + N_{bin,in}^{AB}(\underline{b})} \left\{ -i\tau \langle N_{ch}^{NN} \rangle - \frac{\tau^2}{2} \langle N_{ch}^{NN2} \rangle \right\}$$

$$- \delta(N_{ch}) \int d^2b e^{-N_{bin,in}^{AB}(\underline{b})}$$

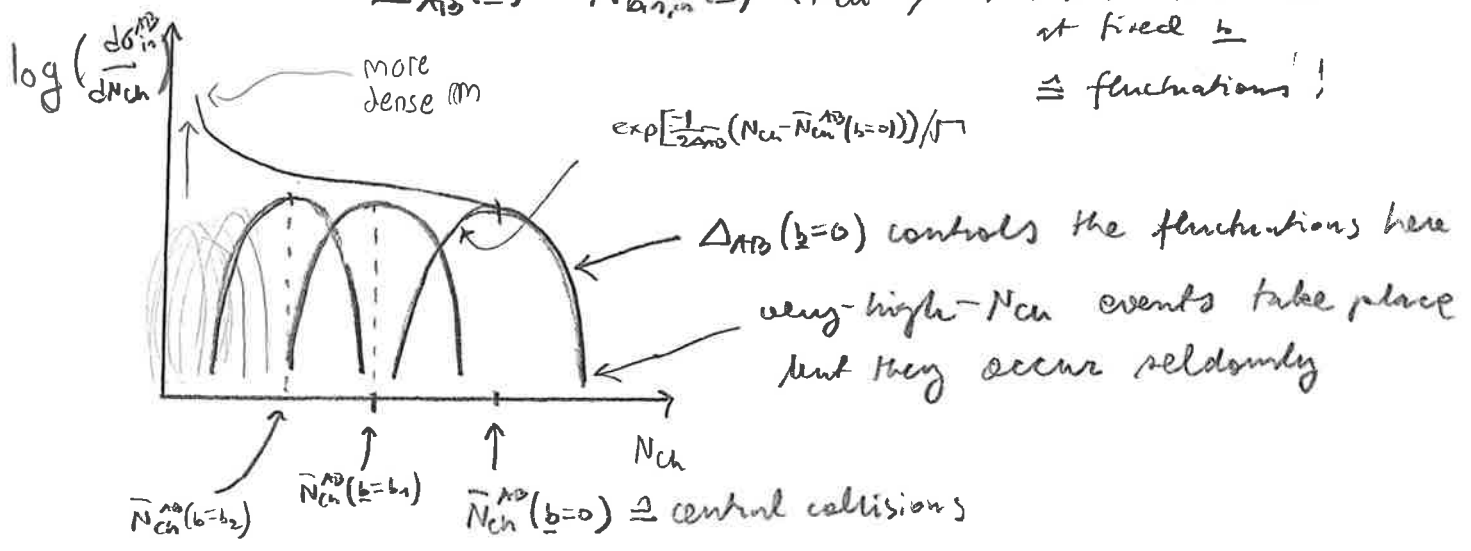
the remaining integral $d\tau$ is Gaussian and doable (E.A.)

$$\Rightarrow \frac{dG_{in}^{AB}}{dN_{ch}} = \int \frac{d^2b}{\sqrt{2\pi} \Delta_{AB}(\underline{b})} e^{-\frac{(N_{ch} - \bar{N}_{ch}^{AB}(\underline{b}))^2}{2\Delta_{AB}(\underline{b})}} - \delta(N_{ch}) \int d^2b e^{-N_{bin,in}^{AB}(\underline{b})}$$

where $\bar{N}_{ch}^{AB}(\underline{b}) = N_{bin,in}^{AB}(\underline{b}) \langle N_{ch}^{NN} \rangle =$ the average # charged hadrons at \underline{b}

$\Delta_{AB}(\underline{b}) = N_{bin,in}^{AB}(\underline{b}) \langle N_{ch}^{NN2} \rangle \rightarrow$ width to the distributions at fixed \underline{b}

\triangleq fluctuations!



We now have a feeling of the physical origin of the fluctuations. Similar consideration can be done for the E_T produced, too.

However, also the medium effects must be taken into account!

[Recall: E_T degradation due to $p dV$ work is $\mathcal{O}(3)$ @ RHIC & LHC!]

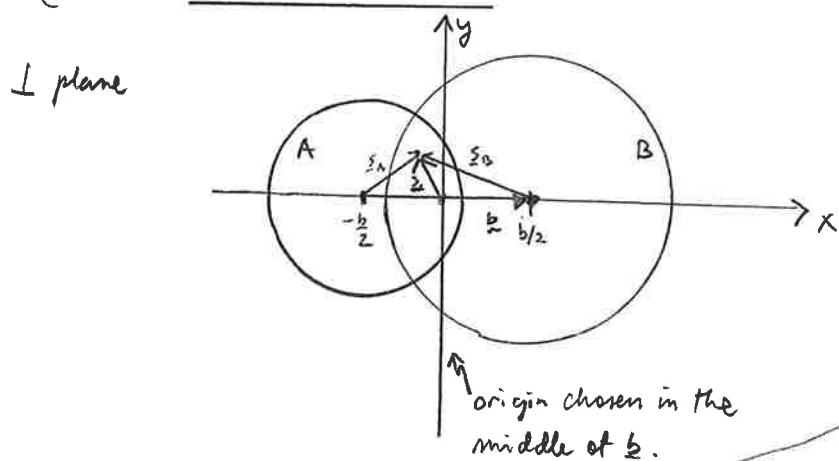
Also, according to the measurements, N_{ch}^{AB} does not scale with the number of binary collisions but, rather, with the number of participants (see later) \Rightarrow the above Glauber-model consideration has to be modified.

Note also that the medium effects are not as drastic for N_{ch} as they are for E_T , since $N_{ch} \propto S_{final} \sim S_{initial}$.

We won't pursue this further here, though.

To understand the classifications of the data better, let's define the

number of participants in an AB collision at fixed b as:
= # of "wounded nucleons"



$$\underline{s}_A = \frac{b}{2} + \underline{s}$$

$$\underline{s}_B = -\frac{b}{2} + \underline{s}$$

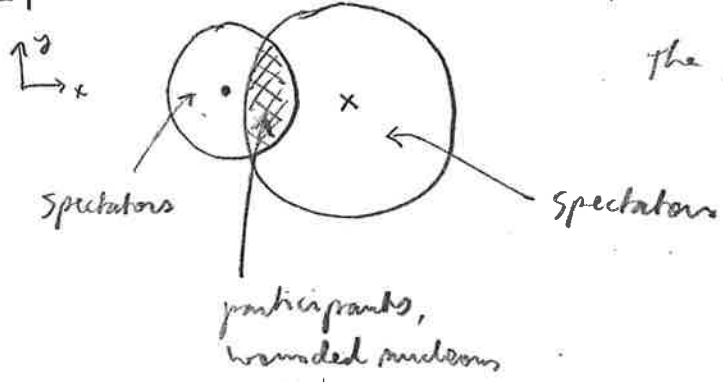
$$N_{part}^{AB}(b) = \int d^2 \underline{s} \left\{ T_A(\underline{s} + \frac{b}{2}) \left[1 - \left(1 - \frac{\sigma_{NN} T_B(\underline{s} - \frac{b}{2})}{B} \right)^B \right] \right. \\ \left. + T_B(\underline{s} - \frac{b}{2}) \left[1 - \left(1 - \frac{\sigma_{NN} T_A(\underline{s} + \frac{b}{2})}{A} \right)^A \right] \right\}$$

$P(\text{at least 1 NN collision in NB})$
 $P(\text{no NN collisions in NB})$
 $P(\text{no NN collisions in NA collision})$
 $P(\text{at least 1 NN collision in NA})$

$d^2 s T_A(\underline{s} - \frac{b}{2})$
 = # nucleons in the $d^2 s$ tube at \underline{s} .

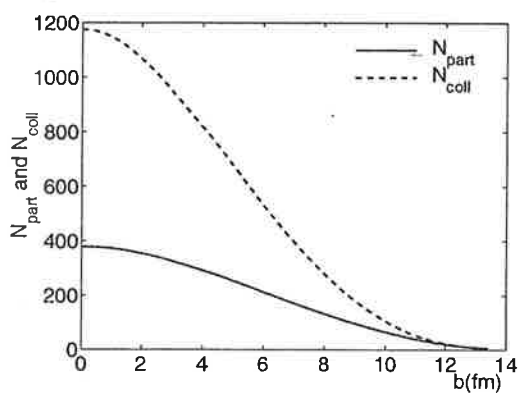
For nuclei with sharp edges, N_{part} gives the amount of nuclear matter in the overlap region.

⊥ plane:



the rest of the nucleons are referred to as "spectators". (*)

Note, however, that the term on p.188 accounts for all \underline{s} when $n_A(r)$ has a tail.



Kolb et al.
hep-ph/0103234

← Computed with Woods-Saxon $n_A(r)$ (p.181)

← $N_{coll} = N_{bin}^{AB}(b) = T_{AB}(b) \sigma_{NN}$

FIG. 1. Number of participating ("wounded") nucleons and of binary nucleon-nucleon collisions as functions of impact parameter. This and all following figures refer to Au+Au collisions at $\sqrt{s} = 130$ A GeV.

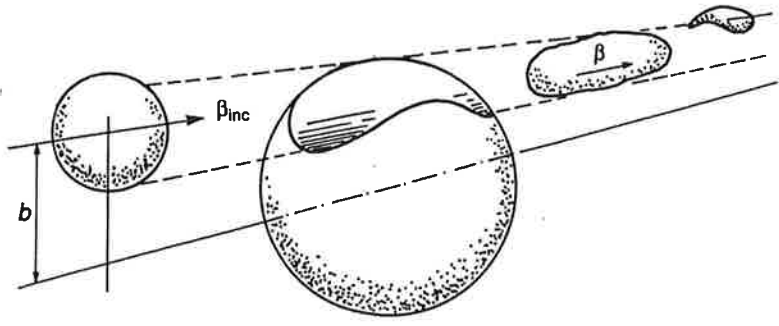
At $A, B \gg 1$, we can again write Poissonian expression:

$$N_{part}^{AB}(b) = \int d^2 \underline{s} \left\{ T_A(\underline{s} + \frac{b}{2}) (1 - e^{-T_B(\underline{s} - \frac{b}{2}) \sigma_{NN}}) + T_B(\underline{s} - \frac{b}{2}) (1 - e^{-T_A(\underline{s} + \frac{b}{2}) \sigma_{NN}}) \right\}$$

from which we see that at the limit $\sigma_{NN} \xrightarrow{\sqrt{s} \rightarrow \infty} \infty$, $N_{part}^{AB} \rightarrow A+B$.

above, $\sigma_{NN}(\sqrt{s}=130 \text{ GeV}) = 40 \text{ mb} \Rightarrow T_{A,B} \sigma_{NN} \gg 1$ until large \underline{s}

$\Rightarrow N_{part}^{AB}(b=0) \approx 197 + 197 \approx 400$
(see the fig.)



(*)
← a fancier figure...

Figure 1.3 Spectators and participants in a heavy ion collision.

7. Non-central collisions at RHIC - some physics results

A. Multiplicity & Hydrodynamics @ RHIC

The 4 experiments at RHIC have measured the following centrality dependence of multiplicity:

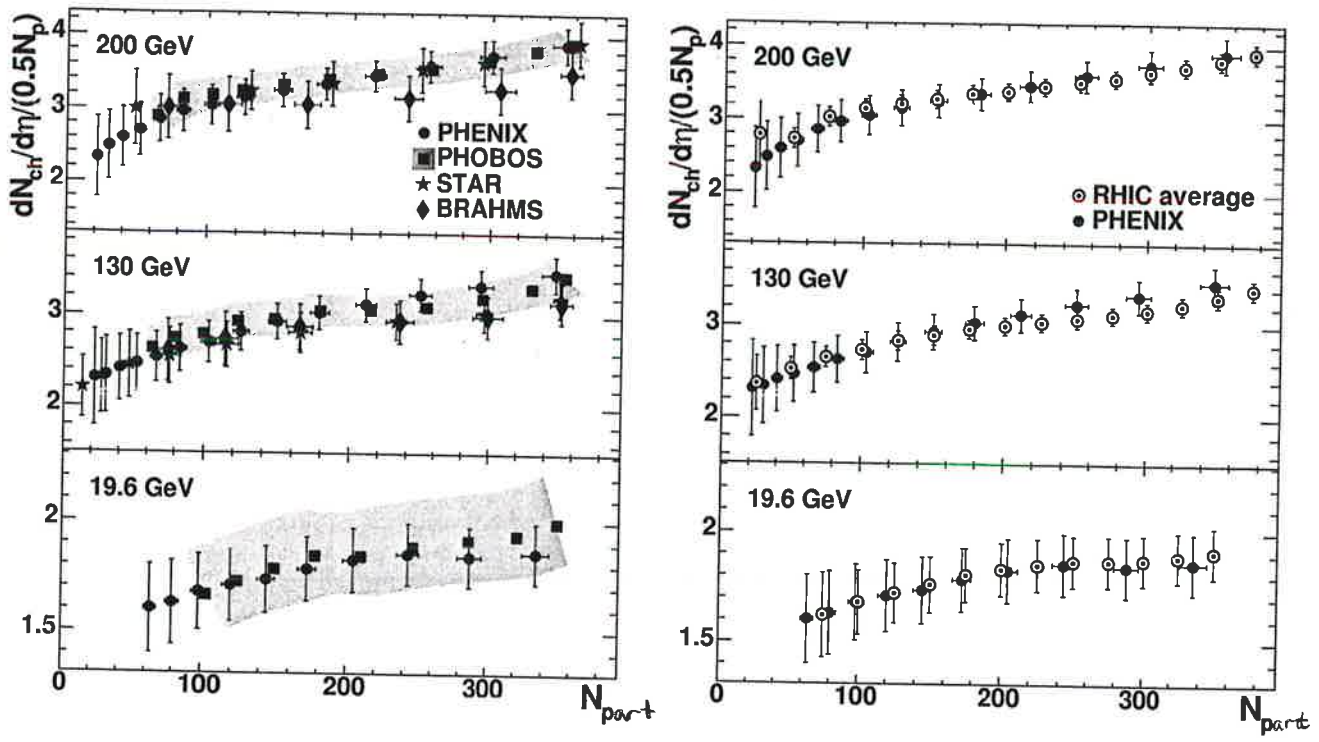


FIG. 9: Left panel: $dN_{ch}/d\eta$ per pair of N_p measured by the four RHIC experiments at different energies. The shaded area is the PHOBOS systematic error. Right panel: RHIC average values (including PHENIX) compared to the PHENIX results.

Thus, near $b \rightarrow 0$ ($N_{part} \rightarrow 100$) $N_{ch} \sim N_{part}$ (roughly).

Hydrodynamical description of the above data includes an assumption at the initial profile, if no ^{specific} model for the initial state is applied. One may try the following possibilities:

1) SWN: Scale the initial entropy density profile with N_{part} :

$$\rho(\underline{s}, \tau_0, b) = K_S \cdot \frac{dN_{part}^{AB}(b)}{d^2s}$$

\nwarrow a fit parameter; obtained from N_{ch} data
 \swarrow the integrand from p. 186

for $P = \frac{1}{3}\epsilon$ ($B=0$), $n_B=0$, we would have $\rho_q = \frac{4}{3} a_q T^3$ shear! \downarrow
 $\Rightarrow \epsilon_q = a_q T^4 = a_q \left(\frac{3}{4} \frac{\rho_q}{a_q} \right)^{4/3}$ which is not $\propto \frac{dN_{part}^{AB}(b)}{d^2s}$ but $\propto \left(\frac{dN_{part}^{AB}(b)}{d^2s} \right)^{4/3}$